Proceedings of the Twenty-first (2011) International Offshore and Polar Engineering Conference
Maui, Hawaii, USA, June 19-24, 2011

ISBN 978-1-880653-96-8 (Set); ISSN 1098-6189 (Set); www.isope.org

Effect of the Sea Level Variation on Storm Surge in the East China Sea

J Li[1], *L. Du*[1*], *J.-C., Zuo*[2], *Y.-F., Yu* [1], *F. Han*[1]
[1] College of Physical and Environmental Oceanography, Ocean University of China
Qingdao, Shandong, China
[2] Key Laboratory of Coastal Disaster and Defence, Ministry of Education, Hohai University
Nanjing, Jiangsu, China

ABSTRACT

A three-dimensional high-resolution hydrodynamic model (ECOMsed) was used to analyze the effects of sea level variations on the storm surge and the check water levels along the coast of East China Sea (ECS). Based on IPCC AR4 A1B scenario, the sea level inter-annual variation with 4-8 years period performed noticeably in middle of the 21st century, and sea level reached the highest level in the 2060 year. The "nominal storm surge" combined with the relevant monthly sea level in the 2060 year in 21st century was simulated in the East China Sea (ECS) by 1989-2008 typhoon cases. The model results exhibited that sea level variations play a significant role on storm surge evolution. Residual elevation difference performed 10 cm in the three tide gauges, and equated to the one fifth of the ECS sea level variability. The influence of sea level variations mapped the geographical variability. The elevation range and the maximal residual elevation increased along the northern coastline of the Jiangsu province and Liaodong Peninsula. The check water level in the ECS coast could reach to 4.5m in 21st century.

KEY WORDS: storm surge; sea level variations; East China Sea; IPCC A1B scenario.

INTRODUCTION

The climate change and the rising sea level are concerned by the international governments and scientists nowadays. As human activities influence on marine and atmospheric processes, the sea level variations become the major issues. There will be more than millions of people suffered from the sea level rise in the eighty decade of 21st century, reported in the IPCC Fourth Assessment Report (IPCC, 2007). Storm surge disaster resulted in huge casualties and enormous economic loss along China coastal area in the last decades. With the development of social industry and agriculture and so as the increase in infrastructure, the disaster loss would be heavier in storm surge. Then, it is an important issue in understanding storm surge change with consideration of sea level variations.

The storm surge elevation is affected by changing topography, and the nonlinear interaction between the tidal and storm surge (Duan et al., 2005; Jiang and Sun, 2002; Huang and Deng, 2007). Former research mainly focused on the effects of long-term sea-level variation on check water levels of multiyear return periods (Du et al., 2007). Yu et al. (2007) simulated tide waves with 1 m mean-sea-level rise, and they presented that the astronomical tidal elevation could change 12-16 cm. Gao et al. (2008) discovered that the surge elevation changed little with mean sea level rise and differed non-uniformly on 5 tide gauges during the three different typhoon cases.

Woodworth and Blackman (2002) concluded that the annual maximum surge-at-high-water was larger in the late 18th, late 19th and late 20th centuries than for most of the 20th century, qualitatively consistent with the long-term variability in storminess from meteorological data. It was reported that the future tropical cyclones (typhoons and hurricanes) will become more intense. Some delta region in Asia will be threat by more storm surge attributed to the sea level rise (IPCC, 2007). Based on the assessment results of IPCC AR4 relative sea level (RSL) rising, Liu (2004) reported storm surge would stronger due to higher RSL and more tropical cyclones. Cui and Shi (2001) found that intensity of storm surges in the China seas increased, although less surges was observed in the 1990's.

Former analysis focused on the effect of sea-level rise on storm surge. The sea-level variations consist of seasonal, inter-decadal and secular variations. Therefore, these remarkable variations should be considered in storm surge research. In these numerical simulations, the sea level during every typhoon seasons, especially from May to October, act as an important indicts. The influence of sea level variations on storm surge in the East China Sea (ECS) was illustrated considering of the IPCC SERS A1B scenario (IPCC, 2007).

DATA AND MODEL

Data

Our storm surge simulation in ECS (117-131°E, 24-41°N) used the high resolution topography data which was interpolated from the measuring data provided by the Chinese Navy. The 4-time daily sea level pressure

* Corresponding author: Du Ling,

(SLP) and wind reanalysis data from the National Centers for Environmental Prediction (NCEP) were provided by the NOAA/OAR/ESRL PSD, Boulder, Colorado, USA, from their web site (http://www.cdc.noaa.gov/). Resolutions of SLP and wind data are 2.5°×2.5° and 1.904°×1.875°, respectively.

Tide elevation data (from National Marine Data & Information Service, State Oceanic Administration) recorded the 20-year annual extreme water level events. Fig. 1 showed the paths of 17 typhoon cases during the annual extreme events (Table 1). There were no selected typhoon cases during three annual extreme events in 1995, 1998 and 1999. Typhoon information during 1989-2005 was supplied by State Oceanic Administration, and the others (from 2006 to 2008) were provided by the Joint Typhoon Warning Center (JTWC) in Naval Oceanography portal (http://www.usno.navy.mil/JTWC/). The typhoon information contains the location, pressure and the maximum wind speed of typhoon center.

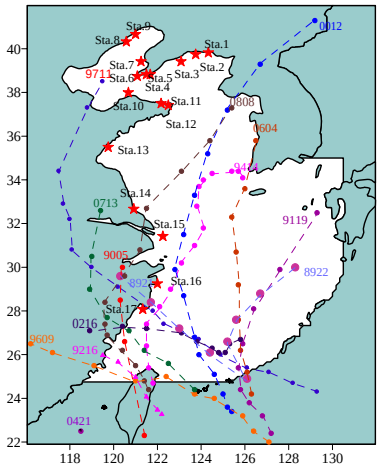

Fig. 1 Typhoons path in the numerical ECS domain mentioned in Table 1 (The typhoons cases named as the 9316#, 0111#, 0316# and 0511# were out of the simulation domain of the ECS, stars presented the location of the gauge stations in the Table 2).

The monthly sea surface heights above geoid were cited from the CCSM 720 PPM stabilization experiment results under the IPCC AR4 SERS A1B scenario. The A1 storyline and scenario family describes a future world of very rapid economic growth, global population that peaks in mid-century and declines thereafter, and the rapid introduction of new and more efficient technologies, where A1B is a balance across all sources in the energy system (IPCC, 2007).

Table 1. Information of the selected typhoon cases

Year	Selected Typhoon	Selected Period	Year	Selected Typhoon	Selected Period
1989	8921	09.15-09.18	1999	--	05.16-05.19
1990	9005	06.23-06.26	2000	0012	08.29-09.01
1991	9119	09.24-09.27	2001	0111	08.19-08.22
1992	9216	08.30-09.02	2002	0216	09.06-09.09
1993	9316	09.15-09.18	2003	0316	09.26-09.29
1994	9414	08.08-08.11	2004	0421	09.13-09.16
1995	--	07.11-07.14	2005	0511	08.19-08.22
1996	9609	07.30-08.02	2006	0603	07.08-07.11
1997	9711	08.17-08.20	2007	0713	09.18-09.21
1998	--	07.23-07.26	2008	0807	07.18-07.21

Description of ECOMsed Model

ECOMsed is a fully integrated three-dimensional hydrodynamic, wave and sediment transport model, which is capable of simulating the sea level, currents, temperature, salinity, wave, transport and fate of suspended sediments, dissolved tracers and neutrally-buoyant particles in estuarine and coastal ocean systems. Several optional modules of ECOMsed consist of the hydrodynamic, sediment transport, wind induced wave, heat flux and particle tracking module. The hydrodynamic, wave and sediment transport model is governing on σ coordinate system. Turbulence closure model takes into consideration of the vertical mixing processes. The detail information refers to the model manual (Blumberg, 2002).

Composited Wind Field with Typhoon

A well wind field with typhoon case is the key trigger to storm surge simulation. Jelesnianski moving typhoon system is widely used to describe the typhoon wind field and its movement. The improved Jelesnianski moving typhoon system consists of circular typhoon component and the additional component caused by the evolution of the cyclonic wind structure. The composited wind field with typhoon is derived from embedding the Jelesnianski moving typhoon system into the NECP wind field.

$$\begin{cases} V_x = \dfrac{r}{R_m + r} V_{cx} - V_m \left(\dfrac{r}{R_m}\right)^{3/2} \dfrac{1}{r}\left(y\cos\varphi + x\sin\varphi\right) \\ V_y = \dfrac{r}{R_m + r} V_{cy} - V_m \left(\dfrac{r}{R_m}\right)^{3/2} \dfrac{1}{r}\left(x\cos\varphi - y\sin\varphi\right) \end{cases} \quad (r \le R_m)$$

$$\begin{cases} V_x = \dfrac{r}{R_m + r} V_{cx} - V_m \left(\dfrac{r}{R_m}\right)^{1/2} \dfrac{1}{r}\left(y\cos\varphi + x\sin\varphi\right) \\ V_y = \dfrac{r}{R_m + r} V_{cy} - V_m \left(\dfrac{r}{R_m}\right)^{1/2} \dfrac{1}{r}\left(x\cos\varphi - y\sin\varphi\right) \end{cases} \quad (r > R_m)$$

Where, (x, y) are the location of model grid; (V_{cx}, V_{cy}) are the velocity component of typhoon center in x, y direction, respectively. φ is the wind influx angle; R_m is the radius of the maximum wind speed; V_m is the maximum wind speed of typhoon.

The corresponding pressure flied, similar with wind field,

$$P_a = P_0 + \frac{1}{4}(P_\infty - P_0)\left(\frac{r}{R_m}\right)^3 \quad (r \le R_m)$$

$$P_a = P_\infty - \frac{3}{4}(P_\infty - P_0)\left(\frac{R_m}{r}\right) \quad (r > R_m)$$

where, P_0 is air pressure of typhoon center, P_a is the calculated air pressure, and P_∞ is environmental air pressure.

RESULT AND DISCUSSION

Simulation Procedure and Validation

Numerical grid of the ECS simulation domain was divided into the resolution of 5′×5′ horizontally and 10 layers vertically. The bottom friction coefficient acted as 0.0025 in the Yellow Sea and the East Sea, 0.0016 in the Bo Hai Sea (Lv and Zhang, 2006).

Table 2. The difference of principal semidiurnal and diurnal tide waves between simulation and observation in the ECS

Sta.	Lon	Lat	M_2		K_1	
			Δamp[b)]	Δpha	Δamp	Δpha
1	124.33	39.83	1.5	13.1	-6.3	1.9
2	123.75	39.75	3.8	8.5	-7.5	-3.6
3	123.08	39.42	6.6	10.4	-7.6	4.4
4	121.67	38.83	-2.2	5.7	-4.3	5.0
5	121.50	38.83	-5.7	-6.9	-5.8	2.5
6	121.08	38.75	-2.3	9.0	-9.1	3.6
7	121.25	39.42	5.2	-3.7	-1.5	1.0
8	121.00	40.67	0.0	4.3	-3.6	1.8
9	120.58	40.33	3.3	8.0	1.9	-0.3
10	120.67	38.00	7.9	-5.8	2.6	16.3
11	122.17	37.50	-4.2	9.0	-1.2	-2.3
12	122.50	37.42	-7.3	18.8	-0.3	1.1
13	119.75	35.50	17.5	-26.2	0.7	8.5
14	120.92	32.67	10.5	63.0	0.4	26.1
15	122.25	31.42	16.2	70.4	0.4	7.9
16	122.00	29.25	1.3	49.3	5.4	23.3
17	121.33	28.08	10.2	50.5	6.5	28.7
mean and standard deviation			3.7±7.2	16.3±26.4	-1.8±4.6	7.4±10.0
mean and standard deviation without 5 stations[a)]			0.6±6.7	5.9±7.8	-3.5±3.9	2.6±5.1

Note: a) Mean and standard deviation value were calculated except for the selected 5 stations, such as sta. 13, 14, 15, 16 and 17.
b) Δamp (unit: centimeter) and Δpha (unit: degree) indicated the amplitude and phase difference between the simulation results and the observation.

The open lateral boundary for the ECOMsed simulation was fixed along the Taiwan Strait, Tsushima Strait, and Ryukyu Archipelago. Under the radiation boundary condition, the model was driven by tide elevation along the boundary assigned from the harmonic constants of the 4 diurnal and semidiurnal constituents.

$$\zeta = \sum_{i=1}^{I} f_i H_i \cos\left[\omega_i t + (V_0 + u)_i - g_i\right]$$

Where, i represents M_2, S_2, K_1, O_1 respectively; H, g and ω are the harmonic constants (amplitude and phase lag) and frequency of every tidal constituent; f and u is the factor and angle of the nodal collection; V_0 is theoretical phase of the astronomical tide.

We compared the simulated tidal characteristic in the ECS with the observation in 17 tide gauge (Table 2). Semidiurnal tide wave partly propagated northward in Yellow Sea, and the other part of the tide wave rotated counterclockwise and finally arrived at the Taiwan Strait, then established four semidiurnal tidal systems with amphidromic points. Our simulation results illustrated the main feature of the tide waves, except for the Korean Peninsula which may be caused by the unrealistic bathymetry and lack of accurate topography data. The simulated amplitude of K_1 tide wave was better than that of the M_2 wave, with the mean difference is -1.8 cm and 3.7 cm. The phase of principal semidiurnal (M_2) and diurnal (K_1) tide waves in most of the area matched well with the observed data, but there was a slight difference with the tide gauge stations in south region of the East Sea.

The twenty storm surge simulations were conducted in the annual extreme water level events from 1989 to 2008. The storm surge simulations were forced by the composited wind and SLP fields on the ECS bathymetry. The sensible experiment result of the 0807# storm surge case in 2008 at the Sta. Qingdao tidal gauge was shown (Fig. 2). The simulated elevations were closed to the observation data, which indicated that the hydrodynamic ECOMsed model could exhibit the ECS storm surge.

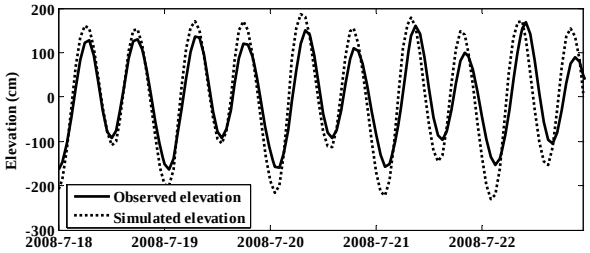

Fig. 2 Simulated and observed elevation in the Sta. Qingdao during the 0807# typhoon case.

Sea Level Variation in the 21st Century

In this section, we investigated the sea level variation, using the SRES A1B scenario recommended by the IPCC AR4, in order to certify the variability of sea level in the 21st century.

Fig. 3 was the CCSM sea level variations in Northwestern Pacific Ocean during 2000-2099 Simulated under the SRES A1B Scenario. The sea level had distinct seasonal, inter-annual and decadal variability, superimposed with secular trend. The annual sea level range was about 10 cm. The annual highest variability appeared in September, while the lowest was in March; it may attribute to the thermal expansion, heat flux in sea surface and wind variability. Besides that, the sea level variations had a noticeable period of 4-8 year in 2030-2060 through the wavelet power spectrum (Fig. 4), which may indicate the influence of the El Niño/LaNina events. The sea level rose gradually from 2000s to 2060s with a rise rate of 2.7 mm/year, and achieved the highest level (51 cm) in the 2060, which may due to the accumulated effects of the individual climate contributors in the 20th century. After that, the sea level descended with a rate of 4.8 mm/year in the next 20 years. It indicated that adaptation strategy already affected on climate change under the A1B scenario when all sources in energy system balanced each other, with assumption of improvement rates applying to all energy supply and end use technologies.

The sea level variations played a significant role in the ocean-atmosphere system. It is found that the tidal waves would change as mean sea level rise (Du et al., 2005; Yu et al., 2007). Thus, we analyzed the storm surge considering the sea level variations under the SRES A1B scenario, in order to examine its influence on coastal ocean processes (shown in next section).

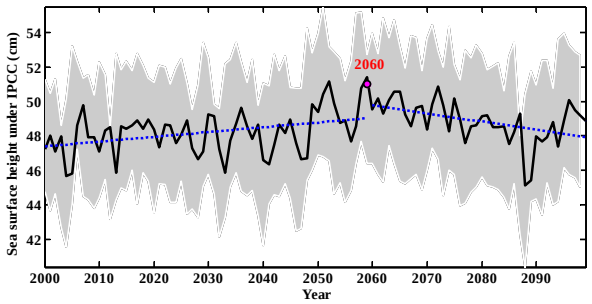

Fig. 3 Sea level in the northwestern Pacific Ocean under the IPCC SRES A1B Scenario in the 21st century (solid line was the annual mean sea level, gray area represented the annual sea level range, dotted lines were the secular trend of sea level).

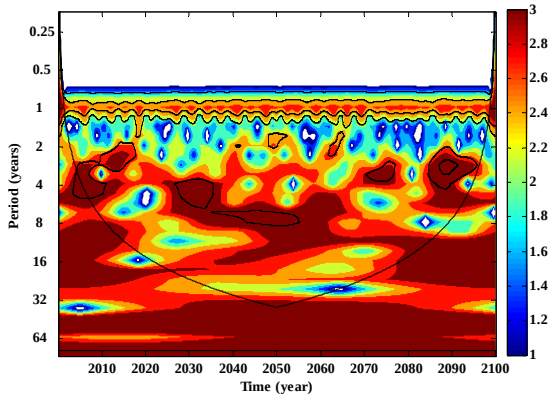

Fig. 4 Wavelet power spectrum of sea level variation under IPCC SERS A1B.

Storm Surge Cases with Sea Level Variations

Hydrodynamic characteristics of the extreme elevations combined with a storm residual elevation were mainly determined by atmospheric disturbance, topography feature and ocean-land distribution, since astronomical tides, storm surge, and their interaction control jointly the real elevation evolution. Large residual elevations were always found in the storm surge disasters. The residual elevations were calculated by subtracting the tidal elevation from the numerical elevation in this paper. Thus, we analyzed the residual elevation variation in order to examine the influence of sea level variation during the 21st century on storm surge simulation in this section.

We simulated the storm surge considering the sea level variations in the 21st century, which named the "nominal storm-surge" case. Since sea level reached the highest level in the 2060 year (Fig. 3), the nominal cases were simulated by the relevant monthly sea level in the year. For example, the nominal 0807# case was simulated with the new bathymetry composed the sea level in August 2060, combined with the similar atmospheric forcing and open boundary condition of the 0807# storm surge case. Thus, the two kinds of cases indicated the influence of sea level variation on the storm surge.

The 0807 typhoon landed at Xiapu (121.4ºE, 28.2ºN), Fujian province at 18:00 of July 18th, and later disturbed the hydrological conditions along the coast of the Zhejiang province and Shanghai. At 2:00 of July 20th, it weakened as a cyclone, going forward to the Yellow sea. Before typhoon arrived, storm set-up occurred in tide ebbing, and increased to high value around the higher tidal water (HTW) until the typhoon system covered the gauges. Then, the highest elevation of the case appeared. After that, the storm set-up occurred during the tide flooding (Fig. 5).

Sea level variations affected the evolution of storm surge. Residual elevation difference between the 0807# case and the nominal- 0807 case illustrated the set-up (set-down) evolution affected by the sea level variations (Fig. 5). Residual elevation difference performed 10 cm in the selected three tide gauges. Residual elevation variation corresponded to the one fifth of the ECS sea level variability of. Compared with the 0807# storm case, we found that residual elevation in the nominal case increased around HTW before the typhoon arrived. It meant that it would extend the storm set-up evolution. Residual elevation difference varied with the semidiurnal tidal current.

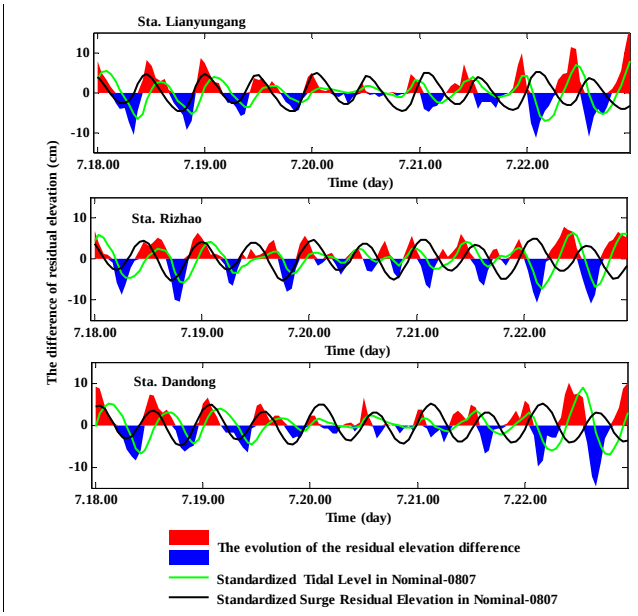

Fig. 5 The evolution of the residual elevation difference between nominal-0807# and 0807# case under sea level variation (the red and blue shaded patch); the standardized tidal level (green line) and the standardized residual elevation (black line) in nominal-0807# case at the three gauges (Sta. Lianyungang (34º45´N, 119º25´E); Sta. Rizhao (35º23´N, 119º32´E); and Sta. Dandong (124º24´E, 40º07´N)).

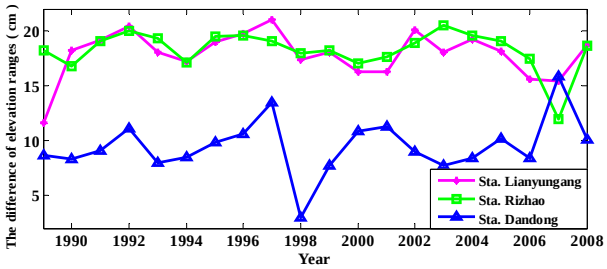

Fig. 6 The difference of elevation ranges between "storm surge" and "nominal-storm surge" of twenty cases in gauge stations.

The sea level variations influenced the storm surge in different way for every storm surge case and mapped the geographical variability. The elevation ranges in the Sta. Lianyungang and the Sta. Rizhao had increased about 20cm in the 20 nominal cases, while it had increased about 10cm along the southeastern coast of the Liaoning Province, such as the Sta. Dandong (Fig. 6).

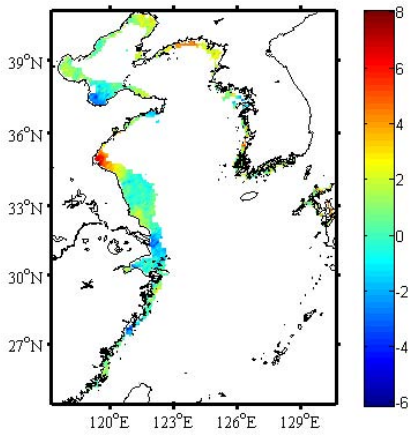

Fig. 7 The difference in the maximal residual elevation between "storm surge" and "nominal-storm surge" in the 21st century in ECS (unit: centimeter).

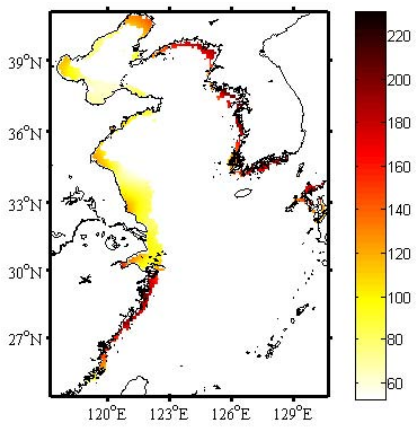

Fig. 8 The average elevation of the maximal residual elevation in the 20 nominal cases (unit: centimeter).

Meanwhile, the maximal residual elevation changed with the effect of the sea level variations. The maximal residual elevation would increase along the northern coastline of the Jiangsu province, and Liaodong Peninsula (Fig. 7). It illustrated the vulnerability along coastline affected by sea level variations in the 21st Century in ECS, which indicated the increasing storm damage in the sensitive area with sea level variations. Generally speaking, the simulation results shown in Fig. 7 were similar to the costal vulnerability in China's National Assessment Report of Climate Change (2007). The north Jiangsu shoal, Bohai coast and Liaodong Peninsula with costal vulnerability would encounter a serious challenge. The maximal residual elevation in the 21st century would occur along the Fujian and Zhejiang province coast, north Jiangsu shoal, Bohai sea western coast, the Liaodong Bay, and eastern coast of the Liaodong Peninsula in ECS (Fig.8). The coastal in Fujian and Zhejiang province were the most seriously area, though north Jiangsu shoal and Bohai coast would be the sensitive area.

Check Water Levels with Sea level Variations

The nominal check water levels of 100-year return period are calculated according to Gumbel extreme distribution law with the 20 nominal cases. The check water level in the 21st century became higher with sea level variations, especially in Zhejiang and Fujian province coast, which simulated with the nominal storm surge cases (Fig. 9). The check water level could reach to 4.5 m along Zhejiang and Fujian provinces coast, while it was 5 m near Changjiang delta, especially at estuary of Qiantangjiang River, and it was 4.5 m along the eastern coast of Liaodong Peninsula. As the tidal distribution pattern change, the check water level was 3 m or more in southern coast of Shandong. Check water level of different return period in 21st century were shown in Fig. 10. The mean check water level of 100-year return period was about 3 m, and it could reach to 7 m in Sta. 1 and 17 especially. The check water level of 100-year return period was higher than that of 20-year return period about 0.7 m. It is important for the coastal engineering.

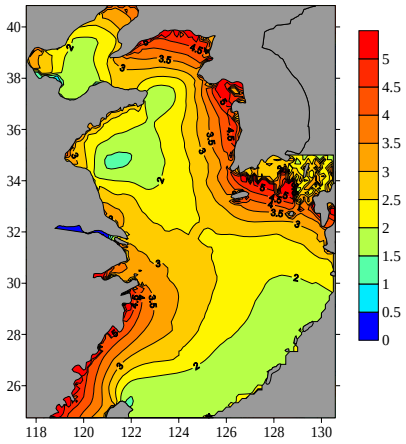

Fig. 9 ECS nominal check water level of 100 year return period in 21st century (unit: meter)

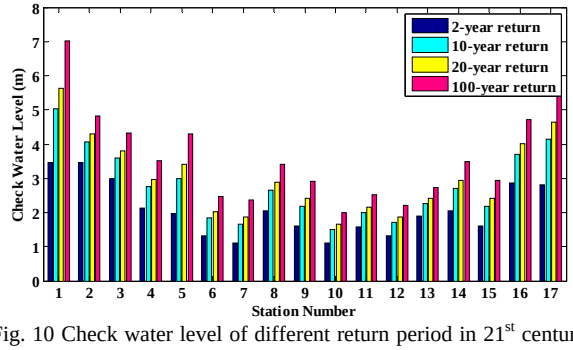

Fig. 10 Check water level of different return period in 21st century (the location of the 17 stations were shown in Fig. 1 by stars)

CONCLUSIONS

Using a fully integrated three-dimensional hydrodynamic model, ECOMsed, we examined effects of the sea level variations on storm surge and check water levels in 21st century on the East China Sea (ECS) considering of the IPCC SERS A1B scenario.

The sea level in 21st century show complicated variations, with seasonal, inter-annual and decadal period for IPCC AR4 A1B scenario. The the annual sea level range was about 10 cm. The inter-annual variation with 4-8 years period performs noticeably. The sea level could reach the highest level (51 cm) in the 2060, after that the sea level will fall slightly.

The simulated results that exhibited the tidal characteristic in the ECS are similar with the observation, and the elevations in storm surge were closed to the observation data. The hydrodynamic ECOMsed model can be used to examine the influence of sea level variations on the storm surge simulation.

Sea level variations affected the evolution of storm surge in 21st century under IPCC AR4 A1B scenario significantly. Storm set-up occurred in tide ebbing before typhoon arrived, and increased to high value around the higher tidal water (HTW) until the typhoon system covered the gauges. Residual elevation difference performed 10 cm in three tide gauges. Residual elevation variation equated to the one fifth of the variability. Sea level variations would extend the storm set-up evolution. Residual elevation difference varied with the semidiurnal tidal current.

The sea level variations influenced the storm surge and mapped the geographical variability. The elevation ranges increased in north Jiangsu shoal and southeastern coast of the Liaoning Province, besides, it increased larger in north Jiangsu shoal. The elevation ranges increased about 20cm in the Sta. Lianyungang and 10cm along the Sta. Dandong.

The maximal residual elevation and check water levels changed with the effect of the sea level variations. The maximal residual elevation will increase along the northern coastline of the Jiangsu province, and Liaodong Peninsula. The check water in the 21st century became higher as sea level varying, especially in Zhejiang and Fujian province coast could reach 4.5 m.

Our result showed that sea level variations made a significant impact on storm surge and check water levels. As the nonlinear interaction of topography, tidal and storm surge, we will further investigate sea level variations affected coastal vulnerability with high resolution land altitude.

ACKNOWLEDGEMENTS

This study is supported by the NSFC project Nos. 40906002, 40806072, 40976006 and 40830746, the Key Scientific Research Program (No. 2007CB411807), the National Key Technology R&D Program (No. 2007BAC03A06) and the project of Key Lab of Coastal Disasters and Defence (No. 200802), and Open Fund of State Key Laboratory of Satellite Ocean Environment Dynamics (No. SOED0905). We appreciate that the North China Sea Marine Forecasting Center of State Oceanic Administration (SOA) and the Joint Typhoon Warning Center (JTWC) in Naval Oceanography portal provide the typhoon information. The NCEP 4-time daily pressure and wind reanalysis data are provided by the NOAA/OAR/ESRL PSD, Boulder, Colorado, USA.

REFERENCES

Blumberg A F (2002). *A primer for ECOMsed, version 1.3*. Mahwah, N J , HydroQual Inc.

Cui CQ, Shi JT (2001).China Coastal Eustatic Change and Storm Surge in the Past Decade. *Marine Science Bulletin*, Vol.20, No.4 pp 20-25.

Du L, Zuo JC, Li L, Li PL, (2005). The Response of Tidal Wave and Engineering Water Level to Long-Term Sea Level Variation in the Jiaozhou Bay. *Proceeding of the fifteenth International Society of Offshore and Polar Engineers (ISOPE-2005) Conference.* Korea, Seoul, ISOPE, vOL 3, pp 713-719.

Du L, Li L, Li PL, Zuo JC, Chen MX (2007).The Calculation of Check Water Levels in the Jiaozhou Bay and Adjacent Sea. *Proceeding of thirteenth International Offshore and Polar Engineering Conference*, Lisbon, Portugal, ISOPE, www.isope.org .

Duan YH, Zhu JR, Qin ZH, Gong MX (2005). A High-resolution Numerical Storm Surge Model in the Changjiang River Estuary and Its Application. *Acta Oceanologica Sinica*, Vol.27, No.3 pp 11-19.

Gao ZG, Han SZ, Liu KX, Zheng YX, Yu HM (2008).Numerical Simulation of the Influence of Mean Sea Level Rise on Typhoon Storm Surge in the East China Sea. *Marine Science Bulletin*, Vol.10, No.2 pp 36-49

Huang LW, Deng J (2007). Response of Yellow and East China Seas to A Typhoon Process. *Oceanologia et Limnologia sinica*. Vol.38, No.3 pp 246-252.

Intergovernmental Panel on Climate Change (IPCC) (2007). *Climate Change 2007: the Physical Science Basis, Summary for Policymakers.* The 10th Session of Working Group I of the IPCC, Paris, February, 2007.

Jiang WS, Sun WX (2002).Simulation of the Iinfluence of the Changing Topography to Storm Surge in Qingdao. *Marine Forecasts*, Vol.19, No.1 pp 97-104.

Liu DJ (2004).Possible Impacts of Relative Sea Level Rise in the Coastal Areas in China. *Marine Forecasts*.Vol.21, No.2 pp 21-28.

Lv XQ, Zhang JC (2006). Numerical Study on Spatially Varying Bottom Friction Coefficient of A 2D Tidal Model with Adjoint Method. *Continental Shelf Research.* Vol.26, pp 1905-1923.

National Assessment Report of Climate Change committee (2007). China's *National Assessment Report of Climate Change*. Science Press. 422 pp.

Woodworth, PL, and DL Blackman (2002). Changes in Extreme High Waters at Liverpool Since 1768. *Int. J. Climatol.*, Vol.22, No.6, pp 697–714.

Yu YF, Liu L, Guo MK (2007).Numerical Research on Tidal Waves Changes Due to Mean-Sea-Level Rise in the Bohai Sea, the Huanghai Sea and the East China Sea: Numerical Modeling of Tidal Waves after Mean-Sea-Level Rise in the Areas. *Periodical of Ocean University of China*.Vol.37,No.1 pp 007-014.